J. Fluid Mech. (2015), *vol.* 784, *pp.* 373–395.
doi:10.1017/jfm.2015.582

Radiation of waves by a cylinder submerged in water with ice floe or polynya

Izolda V. Sturova†

Lavrentyev Institute of Hydrodynamics, av. Lavrentyev 15, Novosibirsk 630090, Russia

(Received 16 March 2015; revised 16 September 2015; accepted 2 October 2015;
first published online 4 November 2015)

The problems of radiation (sway, heave and roll) of surface and flexural-gravity waves by a submerged cylinder are investigated for two configurations, concerning; (i) a freely floating finite elastic plate modelling an ice floe, and (ii) two semi-infinite elastic plates separated by a region of open water (polynya). The fluid of finite depth is assumed to be inviscid, incompressible and homogeneous. The linear two-dimensional problems are formulated within the framework of potential-flow theory. The method of mass sources distributed along the body contour is applied. The corresponding Green's function is obtained by using matched eigenfunction expansions. The radiation load (added mass and damping coefficients) and the amplitudes of vertical displacements of the free surface and elastic plates are calculated. Reciprocity relations which demonstrate both symmetry of the radiation load coefficients and the relation of damping coefficients with the far-field form of the radiation potentials are found. It is shown that wave motion essentially depends on the position of the submerged body relative to the elastic plate edges. The results of solving the radiation problem are compared with the solution of the diffraction problem. It is noted that resonant frequencies in the radiation problem correlate with those frequencies at which the reflection coefficient in the diffraction problem has a local minimum.

Key words: ice sheets, surface gravity waves, wave–structure interactions

1. Introduction

In a linear treatment, the problem of oscillations of a submerged body under a free surface and the resulting hydrodynamic loads have been thoroughly studied. A wide range of mathematical techniques were given by Linton & McIver (2001) for the solution of problems involving the interaction of waves with structures. Extensive bibliographical notes were taken in this book. The investigations of wave fluid motions generated by oscillations of a body beneath a floating elastic plate have been begun relatively recently. Practical applications of this problem are related to studying the effect of floating ice-cover and artificial large floating platforms on submerged bodies. At present, all known theoretical studies of the ice-cover effect on the motion of a submerged body have been carried out under the assumptions that the ice cover is homogeneous and unbounded along the horizontal coordinates. A review of these

† Email address for correspondence: sturova@hydro.nsc.ru

investigations can be found in Sturova (2013). The two-dimensional problem of waves generated by a point source pulsating beneath an ice cover in deep water was solved by Savin & Savin (2013).

In reality, sea ice is strongly inhomogeneous in composition and properties (e.g. Squire 2011). The ice floes have finite dimensions. Cracks, polynyas, and hummocks are the characteristic irregularities of dense ice. Radiation of waves by a horizontal cylinder submerged in fluid having mixed boundary conditions on the upper surface were studied by Sturova (2014) for a floating semi-infinite elastic plate, and Sturova (2015) for two semi-infinite elastic plates connected by the vertical and flexural rotational springs as a model of a partially frozen crack in an ice sheet. These two-dimensional problems were solved by the method of matched eigenfunction expansions (MEE) for the velocity potentials. This method is an efficient direct method to study wave interaction with floating flexible structures (e.g. Sahoo 2012). It provides closed form solutions by transforming the boundary-value problem into a linear system of algebraic equations.

The interaction of a submerged cylinder with a floating elastic platform of finite length was considered by Hermans (2014) and Tkacheva (2015). Hermans extended a semi-analytical method he had earlier proposed to solve the problem of the two-dimensional interaction of a plane wave with a floating flexible platform (e.g. Hermans 2004). To determine the velocity potential, he used the integral equation with Green's function that fulfils the free-surface boundary condition. The deflection of the elastic plate was written as a series of exponential functions. As a result, the problem reduced to solving the differential–integral equation for the deflection of the platform. The computations of the hydrodynamic load for a circular cylinder submerged in front of the platform were presented. The solution to this problem with the use of the Wiener–Hopf technique (WHT) will be published by Tkacheva (2015). The calculations of the hydrodynamic load acting on the elliptical cylinder at different positions with respect to the floating platform are given. The advantage of WHT is that it gives an explicit analytical solution and does not require the use of matching conditions. However, this method is more complicated than the one presented here both in the construction of the solution and in the preparation of a computer program.

In this paper, the linear time-harmonic water–wave problem describing small oscillations of a horizontal cylinder is considered for two classes of hydroelastic system. The fluid surface is either open, except for a finite region where it is covered by a thin elastic platform which represents an ice floe, or covered by two semi-infinite thin elastic plates with different properties, except for a finite patch of ice-free water (polynya). In both cases, the fluid domain is of infinite horizontal extent and finite depth. The uniform Euler–Bernoulli elastic thin plates are used. The axis of the cylinder is parallel to the plate edges and the problems are two-dimensional. The solution is written as a distribution of mass sources over the surface of the cylinder and an integral equation is applied for the unknown source strength. The appropriate Green's function is introduced using the method MEE. While the problem regarding the interaction of a submerged cylinder with a floating elastic platform of finite length has been solved previously, the present study shows that this problem is also amenable to the most simple method MEE. Good agreement between the results obtained by the method MEE and WHT was demonstrated by Sturova & Tkacheva (2015). The case of polynya is considered for the first time. The hydrodynamic load (added mass and damping coefficients) and the amplitudes of vertical displacements of the free surface and elastic plates are calculated as functions of the cylinder oscillation frequency and the location of the cylinder with respect to the plate edges.

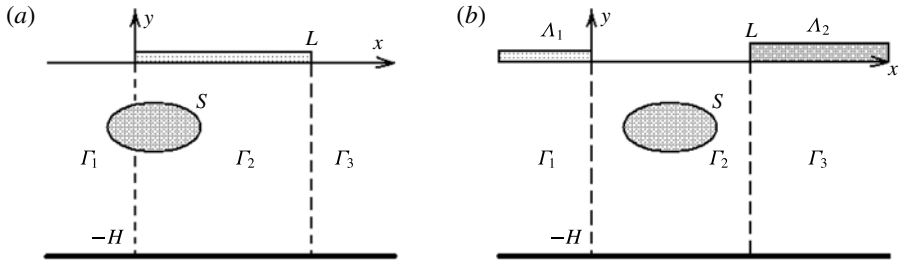

FIGURE 1. Schematic diagram: (*a*) the case of finite elastic platform, (*b*) the case of two semi-infinite elastic plates separated by a region of open water.

The solution of the radiation problem is compared with that of the diffraction problem for the considered elastic plate configurations. It is shown that resonance regimes exist corresponding to local minima of the reflection coefficient in the diffraction problem.

2. Mathematical formulation

The problem is analysed in the 2-D Cartesian coordinate system with the x-axis directed along the undisturbed mean water surface perpendicular to the cylinder axis, and the y-axis pointing vertically upwards. The fluid is assumed to be inviscid and incompressible, its motion is irrotational. The depth of fluid is equal to H. Figure 1 shows a schematic diagram of the problem. The plates are in contact with water at all points for all times. The plate draft is neglected. It is assumed that the edges of plates are free.

Wave motions in the fluid, which is initially at rest, are generated by small horizontal, vertical and rotational oscillations of a submerged rigid body with a wetted surface S. Assuming that the disturbed fluid motion is steady-state, we can write the time-dependent velocity potential under the usual assumptions of linear theory in the form (e.g. Linton & McIver 2001):

$$\Phi(x, y, t) = \mathrm{Re}\left[\mathrm{i}\omega \sum_{j=1}^{3} \zeta_j \varphi_j(x, y) \exp(\mathrm{i}\omega t)\right], \tag{2.1}$$

where complex radiation potentials $\varphi_j(x, y)$ characterize the motion due to body oscillations at a frequency ω with respect to the three degrees of freedom with amplitudes ζ_1, ζ_2 and ζ_3 for the sway, heave and roll problems, respectively, and t is time.

The vertical displacements of the free surface and elastic plates $W(x, t)$ can be determined from the relation

$$\partial W/\partial t = \partial \Phi/\partial y|_{y=0}. \tag{2.2}$$

By analogy with representation (2.1), the expression for $W(x, t)$ can be written in the form:

$$W(x, t) = \mathrm{Re}\left[\sum_{j=1}^{3} \zeta_j w_j(x) \exp(\mathrm{i}\omega t)\right], \quad w_j(x) = \partial \varphi_j/\partial y|_{y=0}. \tag{2.3}$$

The radiation potentials $\varphi_j(x, y)$ satisfy the Laplace equation in the fluid domain

$$\nabla^2\varphi_j = 0 \quad (-\infty < x < \infty,\ -H < y < 0) \tag{2.4}$$

except for the region occupied by the cylinder.

The boundary condition on the closed smooth contour of the submerged body S has the form:

$$\partial\varphi_j/\partial n = n_j \quad (x, y \in S),\ (j = 1, 2, 3). \tag{2.5}$$

Here, $\boldsymbol{n} = (n_x, n_y)$ is the inward normal to the contour S. The notation

$$n_1 = n_x, \quad n_2 = n_y, \quad n_3 = (y - y_0)n_1 - (x - x_0)n_2 \tag{2.6a–c}$$

is used where x_0, y_0 are the coordinates of the centre of roll oscillations.

The boundary condition at the bottom is

$$\partial\varphi_j/\partial y = 0 \quad (-\infty < x < \infty,\ y = -H). \tag{2.7}$$

In the far field, a radiation condition should be imposed that requires the radiated waves to be outgoing.

For a finite platform (see figure 1*a*), the upper boundary of the fluid is covered partly with an elastic homogeneous plate of length L, uniform mass density ρ and thickness d. The fluid surface not covered by the plate is free. The vertical y-axis passes through the left edge of the plate. The free surface condition in the open water regions is given by

$$\partial\varphi_j/\partial y - \Omega\varphi_j = 0, \quad (x < 0, x > L, y = 0),\ \Omega = \omega^2/g, \tag{2.8}$$

where g is the acceleration due to gravity.

On the elastic covered surface, the radiation potentials $\varphi_j(x, y)$ satisfy boundary condition of the form

$$\left(D\frac{\partial^4}{\partial x^4} - \Omega B + 1\right)\frac{\partial\varphi_j}{\partial y} - \Omega\varphi_j = 0 \quad (0 < x < L, y = 0), \tag{2.9}$$

where $D = Ed^3/[12g\rho_0(1 - \nu^2)]$, $B = \rho d/\rho_0$, E is the Young's modulus for the elastic plate, ν is its Poisson's ration and ρ_0 is the fluid density. At the plate edges, free edge conditions require vanishing bending moment and shear force:

$$\partial^3\varphi_j/\partial x^2\partial y = \partial^4\varphi_j/\partial x^3\partial y = 0 \quad (x = 0^+, L^-, y = 0). \tag{2.10}$$

For the polynya of length L (see figure 1*b*), two semi-infinite elastic plates Λ_1 and Λ_2 float on the water surface. The vertical y-axis passes through the right edge of the plate Λ_1. The left plate $\Lambda_1 (x < 0)$ and the right plate $\Lambda_2 (x > L)$ have characteristics E_1, d_1, ρ_1, ν_1 and E_2, d_2, ρ_2, ν_2, respectively. The boundary conditions for the fluid in contact with the plates Λ_1 and Λ_2 are similar (2.9):

$$\left(D_1\frac{\partial^4}{\partial x^4} - \Omega B_1 + 1\right)\frac{\partial\varphi_j}{\partial y} - \Omega\varphi_j = 0 \quad (x < 0, y = 0), \tag{2.11a}$$

$$\left(D_2\frac{\partial^4}{\partial x^4} - \Omega B_2 + 1\right)\frac{\partial\varphi_j}{\partial y} - \Omega\varphi_j = 0 \quad (x > L, y = 0), \tag{2.11b}$$

where $D_n = E_n d_n^3/[12g\rho_0(1 - \nu_n^2)]$, $B_n = \rho_n d_n/\rho_0$ $(n = 1, 2)$. The free edge conditions (2.10) are fulfilled at $(x = 0^-, L^+, y = 0)$. The free surface condition (2.8) takes place at $(0 < x < L, y = 0)$.

3. Method of solution

To solve the Laplace equation (2.4) with the appropriate boundary conditions we introduce an unknown mass source distribution $\sigma_j(x, y)$ over the contour S for each of the body oscillation modes. Then, the radiation potentials at any point of the fluid can be represented in the form

$$\varphi_j(x, y) = \int_S \sigma_j(\xi, \eta) G(x, y; \xi, \eta)\, \mathrm{d}s \quad (j = 1, 2, 3). \tag{3.1}$$

Here, $G(x, y; \xi, \eta)$ is the Green's function which determines the fluid velocity potential initiated by a mass source of unit intensity located at the point with coordinates (ξ, η). In order to determine the Green's function, it is necessary to solve the equation

$$\nabla^2 G = 2\pi\delta(x - \xi)\delta(y - \eta), \tag{3.2}$$

where δ is the Dirac delta-function, with the boundary conditions similar to (2.7)–(2.11) and the radiation condition in the far field.

The Green's function can be found using the method MME. The domain occupied by fluid is divided into three subdomains: $\Gamma_1(-\infty < x < 0, -H < y < 0)$, $\Gamma_2(0 < x < L, -H < y < 0)$ and $\Gamma_3(L < x < \infty, -H < y < 0)$. The value of $G(x, y; \xi, \eta)$ in Γ_i is denoted by $G_i(x, y; \xi, \eta)$ $(i = 1, 2, 3)$. The Green's function depends significantly on the location of the source. The cases of finite platform and polynya will be considered further separately.

3.1. *The Green's function for the case of finite elastic platform*

The functions $G_i(x, y; \xi, \eta)$ $(i = 1, 2, 3)$ will be sought as expansions in terms of eigenfunctions of corresponding boundary value problems:

$$G_1 = \alpha_1 G_f + R_0 \mathrm{e}^{\mathrm{i}k_0 x} f(y, k_0) + \sum_{m=1}^{\infty} R_m \mathrm{e}^{k_m x} \psi(y, k_m) \quad (x, y \in \Gamma_1), \tag{3.3}$$

$$G_2 = \alpha_2 G_p + [C_0 \mathrm{e}^{-\mathrm{i}s_0 x} + S_0 \mathrm{e}^{\mathrm{i}s_0 (x-L)}] f(y, s_0) + \sum_{\substack{m=-2 \\ m\neq 0}}^{\infty} [C_m \mathrm{e}^{-s_m x} + S_m \mathrm{e}^{s_m (x-L)}] \psi(y, s_m) \quad (x, y \in \Gamma_2), \tag{3.4}$$

$$G_3 = \alpha_3 G_f + T_0 \mathrm{e}^{\mathrm{i}k_0 (L-x)} f(y, k_0) + \sum_{m=1}^{\infty} T_m \mathrm{e}^{k_m (L-x)} \psi(y, k_m) \quad (x, y \in \Gamma_3), \tag{3.5}$$

where

$$f(y, k) = \cosh k(y + H)/\cosh kH, \quad \psi(y, k) = \cos k(y + H)/\cos kH. \tag{3.6a,b}$$

The value α_i $(i = 1, 2, 3)$ in (3.3)–(3.5) is equal to one if the observation point (x, y) and the mass source (ξ, η) are located in the same subdomain Γ_i, otherwise $\alpha_i = 0$.

The constants k_m's satisfy the dispersion relations

$$\Omega = k_0 \tanh k_0 H = -k_m \tan k_m H \quad (m = 1, 2, 3, \ldots) \tag{3.7}$$

with $(m - 1)\pi/H < k_m < m\pi/H$ $(m = 1, 2, 3, \ldots)$. The eigenfunctions $f(y, k_0)$, $\psi(y, k_m)$ $(m = 1, 2, 3, \ldots)$ are orthogonal and form the complete system. These

functions are determined by taking (2.4), the boundary conditions (2.7) and (2.8) into account.

Taking into account the boundary condition (2.9), the constant s_m's satisfy the dispersion relation

$$\mathscr{K} = s_0(1 + \mathscr{L}s_0^4)\tanh s_0 H = -s_m(1 + \mathscr{L}s_m^4)\tan s_m H \quad (m = -2, -1, 1\ldots) \tag{3.8}$$

with $\mathscr{K} = \Omega/(1 - \Omega B)$ and $\mathscr{L} = D/(1 - \Omega B)$. It should be noted that s_{-2} and s_{-1} are complex conjugates with positive real parts, s_m's are positive and real with $(m - 1)\pi/H < s_m < m\pi/H$ $(m = 1, 2, 3, \ldots)$. The eigenfunctions $f(y, s_0)$, $\psi(y, s_m)$ $(m = -2, -1, 1, \ldots)$ are not orthogonal, however they do form a complete set (e.g. Fox & Squire 1994).

The function $G_f(x, y; \xi, \eta)$ is a velocity potential due to a source submerged under an infinitely extended free surface (e.g. Linton & McIver 2001, (B.38), (B.40)):

$$G_f = \ln\frac{r}{r_1} + \mathrm{pv}\int_0^\infty P_0(y, \eta; k)\frac{\cos k(x - \xi)}{Z_0(k)}\,\mathrm{d}k - \mathrm{i}\pi P_0(y, \eta; k_0)\frac{\cos k_0(x - \xi)}{Z_0'(k_0)}, \tag{3.9}$$

where 'pv' indicates the principal-value integration,

$$r^2 = (x - \xi)^2 + (y - \eta)^2, \quad r_1^2 = (x - \xi)^2 + (y + \eta)^2, \tag{3.10a,b}$$

$$P_0 = \frac{2}{k(1 + \mathrm{e}^{-2kH})}\{[(k\cosh k\eta + \Omega\sinh k\eta)\mathrm{e}^{-ky} - (\Omega + k)\mathrm{e}^{ky}\sinh k\eta]\mathrm{e}^{-2kH} + k\mathrm{e}^{k(y+\eta)}\}, \tag{3.11}$$

$$Z_0(k) = \Omega - k\tanh kH, \quad Z_0'(k_0) \equiv \mathrm{d}Z_0/\mathrm{d}k|_{k=k_0}. \tag{3.12a,b}$$

The function $G_p(x, y; \xi, \eta)$ represents the velocity potential due to a source submerged beneath an infinitely extended elastic plate:

$$G_p = \ln\frac{r}{r_1} + \mathrm{pv}\int_0^\infty P(y, \eta; k)\frac{\cos k(x - \xi)}{Z(k)}\,\mathrm{d}k - \mathrm{i}\pi P(y, \eta; s_0)\frac{\cos s_0(x - \xi)}{Z'(s_0)}, \tag{3.13}$$

where

$$P(y, \eta; k) = \frac{2}{k(1 + \mathrm{e}^{-2kH})}\left\{k(\mathscr{L}k^4 + 1)[(\mathrm{e}^{-ky}\cosh k\eta - \mathrm{e}^{ky}\sinh k\eta)\mathrm{e}^{-2kH} + \mathrm{e}^{k(y+\eta)}]\right.$$
$$\left. - 2\mathscr{K}\mathrm{e}^{-2kH}\sinh k\eta\sinh ky\right\}, \tag{3.14}$$

$$Z(k) = \mathscr{K} - k(1 + \mathscr{L}k^4)\tanh kH, \quad Z'(s_0) \equiv \mathrm{d}Z/\mathrm{d}k|_{k=s_0}. \tag{3.15a,b}$$

The unknown constants R_m, C_m, S_m, T_m in (3.3)–(3.5) should be determined to obtain the Green's function completely. Since the pressure and horizontal velocity are continuous across the boundary between the subdomains Γ_1 and Γ_2 and also on the boundary between Γ_2 and Γ_3, the full solution can be obtained from matching conditions

$$G_1|_{x=0-} = G_2|_{x=0+}, \quad \partial G_1/\partial x|_{x=0-} = \partial G_2/\partial x|_{x=0+}, \tag{3.16a,b}$$

$$G_2|_{x=L-} = G_3|_{x=L+}, \quad \partial G_2/\partial x|_{x=L-} = \partial G_3/\partial x|_{x=L+} \quad (-H < y < 0). \tag{3.16c,d}$$

In accordance with the radiation condition, in the far field there exist only waves outgoing from the source with wavenumber k_0. In order to determine the behaviour of the Green's function in (3.3) and (3.5) as $x-\xi \to \pm\infty$ it is sufficient to consider only the limiting values of the first terms:

$$G_1 = Q_1(\xi, \eta) f(y, k_0) \mathrm{e}^{\mathrm{i}k_0 x} \quad (x-\xi \to -\infty), \tag{3.17a}$$

$$G_3 = Q_2(\xi, \eta) f(y, k_0) \mathrm{e}^{-\mathrm{i}k_0 x} \quad (x-\xi \to \infty), \tag{3.17b}$$

where

$$Q_1(\xi, \eta) = R_0 - 2\mathrm{i}\pi\alpha_1 \mathrm{e}^{-\mathrm{i}k_0\xi} f(\eta, k_0)/Z_0'(k_0), \tag{3.18a}$$

$$Q_2(\xi, \eta) = T_0 \mathrm{e}^{\mathrm{i}k_0 L} - 2\mathrm{i}\pi\alpha_3 \mathrm{e}^{\mathrm{i}k_0\xi} f(\eta, k_0)/Z_0'(k_0). \tag{3.18b}$$

3.2. *The Green's function for the case of polynya*

The functions $G_i(x, y; \xi, \eta)$ $(i = 1, 2, 3)$ can be sought in the form:

$$G_1 = \alpha_1 G_p^{(1)} + R_0 \mathrm{e}^{\mathrm{i}q_0 x} f(y, q_0) + \sum_{\substack{m=-2 \\ m\neq 0}}^{\infty} R_m \mathrm{e}^{q_m x} \psi(y, q_m) \quad (x, y \in \Gamma_1), \tag{3.19}$$

$$G_2 = \alpha_2 G_f + \left[C_0 \mathrm{e}^{-\mathrm{i}k_0 x} + S_0 \mathrm{e}^{\mathrm{i}k_0(x-L)}\right] f(y, k_0) + \sum_{m=1}^{\infty} \left[C_m \mathrm{e}^{-k_m x} + S_m \mathrm{e}^{k_m(x-L)}\right] \psi(y, k_m) \quad (x, y \in \Gamma_2), \tag{3.20}$$

$$G_3 = \alpha_3 G_p^{(2)} + T_0 \mathrm{e}^{\mathrm{i}p_0(L-x)} f(y, p_0) + \sum_{\substack{m=-2 \\ m\neq 0}}^{\infty} T_m \mathrm{e}^{p_m(L-x)} \psi(y, p_m) \quad (x, y \in \Gamma_3). \tag{3.21}$$

The constant q_m's and p_m's satisfy dispersion relations (3.8) using in place of E, d, ρ, ν the values E_1, d_1, ρ_1, ν_1 and E_2, d_2, ρ_2, ν_2, respectively:

$$\mathscr{K}_1 = q_0(1 + \mathscr{L}_1 q_0^4) \tanh q_0 H = -q_m(1 + \mathscr{L}_1 q_m^4) \tan q_m H, \tag{3.22a}$$

$$\mathscr{K}_2 = p_0(1 + \mathscr{L}_2 p_0^4) \tanh p_0 H = -p_m(1 + \mathscr{L}_2 p_m^4) \tan p_m H \tag{3.22b}$$

with

$$\mathscr{K}_n = \Omega/(1 - \Omega B_n), \quad \mathscr{L}_n = D_n/(1 - \Omega B_n) \quad (n = 1, 2). \tag{3.23a,b}$$

The functions $G_p^{(n)} (n = 1, 2)$ in (3.19) and (3.21) are equal to the function G_p in (3.13) replacing the values $\mathscr{K}, \mathscr{L}, s_0$ by the values $\mathscr{K}_1, \mathscr{L}_1, q_0$ at $n = 1$ and $\mathscr{K}_2, \mathscr{L}_2, p_0$ at $n = 2$, respectively.

The unknown constants R_m, C_m, S_m, T_m in (3.19)–(3.21) can be determined from matching conditions (3.16*a–d*). In the far field, the wave with wavenumber q_0 propagates to the left as $x-\xi \to -\infty$, and the wave with wavenumber p_0 propagates to the right as $x-\xi \to \infty$. The limiting values of the Green's function as $x-\xi \to \pm\infty$ are equal to

$$G_1 = V_1(\xi, \eta) f(y, q_0) \mathrm{e}^{\mathrm{i}q_0 x} \quad (x-\xi \to -\infty), \tag{3.24a}$$

$$G_3 = V_2(\xi, \eta) f(y, p_0) \mathrm{e}^{-\mathrm{i}p_0 x} \quad (x-\xi \to \infty), \tag{3.24b}$$

where

$$V_1(\xi, \eta) = R_0 - 2\mathrm{i}\pi\alpha_1(1 + \mathscr{L}_1 q_0^4) \mathrm{e}^{-\mathrm{i}q_0\xi} f(\eta, q_0)/Z'(q_0), \tag{3.25}$$

$$V_2(\xi, \eta) = T_0 \mathrm{e}^{\mathrm{i}p_0 L} - 2\mathrm{i}\pi\alpha_3(1 + \mathscr{L}_2 p_0^4) \mathrm{e}^{\mathrm{i}p_0\xi} f(\eta, p_0) Z'(p_0). \tag{3.26}$$

3.3. *Integral equation*

Using boundary condition (2.5) on the cylinder surface S, we obtain the following integral equation to determine the source distribution $\sigma_j(x, y)$

$$\pi\sigma_j(x, y) - \int_S \sigma_j(\xi, \eta)\frac{\partial G}{\partial n}\,\mathrm{d}s = n_j \quad (j = 1, 2, 3). \tag{3.27}$$

This is a Fredholm integral equation of the second kind for the source distribution. Once the distribution of the sources $\sigma_j(x, y)$ has been calculated, we can determine the radiation potentials (3.1).

Using (3.17) and (3.24*a*,*b*), we can readily note that the radiation potentials in the far field have the form:

for the case of the platform

$$\varphi_j = A_j^{\pm}\mathrm{e}^{\mp\mathrm{i}k_0 x}f(y, k_0) \quad (x \to \pm\infty), \tag{3.28}$$

for the case of polynya

$$\varphi_j = \begin{cases} E_j^{-}\mathrm{e}^{\mathrm{i}q_0 x}f(y, q_0) & (x \to -\infty), \\ \varphi_j = E_j^{+}\mathrm{e}^{-\mathrm{i}p_0 x}f(y, p_0) & (x \to \infty), \end{cases} \tag{3.29}$$

where

$$A_j^{-} = \int_{S_1} Q_1(\xi, \eta)\sigma_j(\xi, \eta)\,\mathrm{d}s + \int_{S_2+S_3} R_0(\xi, \eta)\sigma_j(\xi, \eta)\,\mathrm{d}s, \tag{3.30}$$

$$A_j^{+} = \mathrm{e}^{\mathrm{i}p_0 L}\int_{S_1+S_2} T_0(\xi, \eta)\sigma_j(\xi, \eta)\,\mathrm{d}s + \int_{S_3} Q_2(\xi, \eta)\sigma_j(\xi, \eta)\,\mathrm{d}s, \tag{3.31}$$

$$E_j^{-} = \int_{S_1} V_1(\xi, \eta)\sigma_j(\xi, \eta)\,\mathrm{d}s + \int_{S_2+S_3} R_0(\xi, \eta)\sigma_j(\xi, \eta)\,\mathrm{d}s, \tag{3.32}$$

$$E_j^{+} = \mathrm{e}^{\mathrm{i}p_0 L}\int_{S_1+S_2} T_0(\xi, \eta)\sigma_j(\xi, \eta)\,\mathrm{d}s + \int_{S_3} V_2(\xi, \eta)\sigma_j(\xi, \eta)\,\mathrm{d}s. \tag{3.33}$$

Here, S_i $(i = 1, 2, 3)$ is the part of contour S located in the subdomain Γ_i.

The vertical displacements of the free surface and elastic plates can be determined from (2.3) and (3.1):

$$w_j(x) = \int_S \sigma_j(\xi, \eta)\left.\frac{\partial G}{\partial y}\right|_{y=0}\mathrm{d}s. \tag{3.34}$$

In accordance with (3.28) and (3.29) in the far field we have:

for the case of the platform

$$w_j = k_0 A_j^{\pm}\mathrm{e}^{\mp\mathrm{i}k_0 x}\tanh k_0 H \quad (x \to \pm\infty), \tag{3.35}$$

for the case of polynya

$$w_j = \begin{cases} q_0 E_j^{-}\mathrm{e}^{\mathrm{i}q_0 x}\tanh q_0 H & (x \to -\infty), \\ p_0 E_j^{+}\mathrm{e}^{-\mathrm{i}p_0 x}\tanh p_0 H & (x \to \infty). \end{cases} \tag{3.36}$$

4. Hydrodynamic load and reciprocity relations

The radiation load acting on an oscillating submerged body is determined by the force $\boldsymbol{F} = (F_1, F_2)$ and the moment F_3 which, without taking account of the hydrostatic term, have the form (e.g. Linton & McIver 2001)

$$F_k = \sum_{j=1}^{3} \zeta_j \tau_{kj} \quad (k = 1, 2, 3),\ \tau_{kj} = \rho_0 \omega^2 \int_S \varphi_j n_k \, \mathrm{d}s = \omega^2 \mu_{kj} - \mathrm{i}\omega \lambda_{kj}. \tag{4.1}$$

The coefficients τ_{kj} represent the complex force acting in the direction k and associated with the sinusoidal motion of the body with unit amplitude in the direction j, and μ_{kj} and λ_{kj} are the added mass and damping coefficients, respectively.

We will derive some general identities relating the quantities that have been introduced. The method of generating these so-called reciprocity relations is well-known for the body submerged beneath an infinitely extended free surface (e.g. Linton & McIver 2001). Let $\vartheta(x, y)$ and $\chi(x, y)$ be two harmonic potentials both satisfying bottom boundary condition (2.7) and surface conditions (2.8)–(2.10) for the case of the elastic platform (or corresponding conditions for the case of polynya). Using the Green's identity for the fluid region outside the submerged body, we obtain

$$\begin{aligned} &\int_S \left(\vartheta \frac{\partial \chi}{\partial n} - \chi \frac{\partial \vartheta}{\partial n} \right) \mathrm{d}s + \int_{-\infty}^{\infty} \left(\vartheta \frac{\partial \chi}{\partial y} - \chi \frac{\partial \vartheta}{\partial y} \right) \Big|_{y=0} \mathrm{d}x \\ &\quad + \int_{-H}^{0} \left(\vartheta \frac{\partial \chi}{\partial x} - \chi \frac{\partial \vartheta}{\partial x} \right) \Big|_{x=-\infty}^{x=\infty} \mathrm{d}y = 0. \end{aligned} \tag{4.2}$$

We denote the second of integrals in (4.2) as

$$I \equiv \int_{-\infty}^{\infty} \left(\vartheta \frac{\partial \chi}{\partial y} - \chi \frac{\partial \vartheta}{\partial y} \right) \Big|_{y=0} \mathrm{d}x. \tag{4.3}$$

For the case of the platform, we have

$$I = \frac{D}{\Omega} \int_0^L \left(\frac{\partial^5 \vartheta}{\partial^4 x \partial y} \frac{\partial \chi}{\partial y} - \frac{\partial^5 \chi}{\partial^4 x \partial y} \frac{\partial \vartheta}{\partial y} \right) \Big|_{y=0} \mathrm{d}x = D[U(L) - U(0)]/\Omega, \tag{4.4}$$

where

$$U(x) = \left[\frac{\partial^4 \vartheta}{\partial x^3 \partial y} \frac{\partial \chi}{\partial y} - \frac{\partial^3 \vartheta}{\partial x^2 \partial y} \frac{\partial^2 \chi}{\partial x \partial y} + \frac{\partial^2 \vartheta}{\partial x \partial y} \frac{\partial^3 \chi}{\partial x^2 \partial y} - \frac{\partial \vartheta}{\partial y} \frac{\partial^4 \chi}{\partial x^3 \partial y} \right]_{y=0}. \tag{4.5}$$

Here, boundary conditions (2.8) and (2.9) are used. Taking free-edge conditions (2.10) into account, we have $U(L) = U(0) = 0$ and hence $I = 0$ in (4.4).

For the case of polynya, we have

$$\begin{aligned} I &= \frac{D_1}{\Omega} \int_{-\infty}^{0} \left(\frac{\partial^5 \vartheta}{\partial^4 x \partial y} \frac{\partial \chi}{\partial y} - \frac{\partial^5 \chi}{\partial^4 x \partial y} \frac{\partial \vartheta}{\partial y} \right) \Big|_{y=0} \mathrm{d}x \\ &\quad + \frac{D_2}{\Omega} \int_L^{\infty} \left(\frac{\partial^5 \vartheta}{\partial^4 x \partial y} \frac{\partial \chi}{\partial y} - \frac{\partial^5 \chi}{\partial^4 x \partial y} \frac{\partial \vartheta}{\partial y} \right) \Big|_{y=0} \mathrm{d}x \\ &= [D_2 U(\infty) - D_1 U(-\infty)]/\Omega. \end{aligned} \tag{4.6}$$

For the functions ϑ and χ, we can take both various pairs of φ_j and their complex conjugate values $\bar{\varphi}_j$. Suppose $\vartheta = \varphi_j$ and $\chi = \varphi_k$ are two radiation potentials

corresponding to two different modes of motion. Then the first integral in (4.2) with using (2.5) and (4.1) is equal to

$$\int_S \left(\varphi_j \frac{\partial \varphi_k}{\partial n} - \varphi_k \frac{\partial \varphi_j}{\partial n}\right) \mathrm{d}s = \int_S (\varphi_j n_k - \varphi_k n_j)\, \mathrm{d}s = \frac{1}{\rho_0 \omega^2}(\tau_{kj} - \tau_{jk}). \tag{4.7}$$

Taking into consideration the behaviour of the radiation potentials in the far field (3.28) and (3.29), we obtain the second and third integrals in (4.2) which are equal to zero. Consequently, the added mass and damping coefficients given by (4.1) are symmetric

$$\mu_{jk} = \mu_{kj}, \quad \lambda_{jk} = \lambda_{kj} \quad (j, k = 1, 2, 3). \tag{4.8a,b}$$

This takes place both in the case of the platform and in the case of polynya.

If we use $\vartheta = \varphi_j$ and $\chi = \bar{\varphi}_k$ in (4.2), then the first integral in (4.2) using (2.5) and (4.1) can be written as

$$\int_S \left(\varphi_j \frac{\partial \bar{\varphi}_k}{\partial n} - \bar{\varphi}_k \frac{\partial \varphi_j}{\partial n}\right) \mathrm{d}s = -\frac{2\mathrm{i}}{\rho_0 \omega} \lambda_{kj}. \tag{4.9}$$

Consequently, we can relate the damping coefficient to the far-field form of the radiation potentials with regard to (3.28) and (3.29): for the case of the platform

$$\lambda_{kj} = \rho_0 \omega k_0 Y(k_0)(A_k^- \bar{A}_j^- + A_k^+ \bar{A}_j^+), \tag{4.10}$$

for the case of polynya

$$\lambda_{kj} = \rho_0 \omega (\Upsilon_1 E_k^- \bar{E}_j^- + \Upsilon_2 E_k^+ \bar{E}_j^+), \tag{4.11}$$

where

$$\Upsilon_1 = q_0[2D_1 q_0^4 \tanh^2 q_0 H/\Omega + Y(q_0)], \tag{4.12a}$$

$$\Upsilon_2 = p_0[2D_2 p_0^4 \tanh^2 p_0 H/\Omega + Y(p_0)], \tag{4.12b}$$

$$Y(\alpha) = \frac{1}{\cosh^2 \alpha H} \int_{-H}^{0} \cosh^2[\alpha(y+H)]\, \mathrm{d}y = \frac{1}{2}\left[H(1 - \tanh^2 \alpha H) + \frac{\tanh \alpha H}{\alpha}\right]. \tag{4.13}$$

From (4.10) and (4.11) it follows that the diagonal damping coefficients are always non-negative. Equation (4.10) is coincident with the reciprocity relation for a body submerged beneath an infinitely extended free surface (e.g. Linton & McIver 2001, equation (1.52)). Equation (4.11) repeats the corresponding relation for a body submerged under an ice cover with a crack (Sturova 2015). These reciprocity relations are useful for testing accuracy in numerical calculations.

5. Numerical results

The calculations are performed for the elliptic contour $S: (x-c)^2/a^2 + (y+h)^2/b^2 = 1$, where a and b are the major and minor axes of the ellipse, respectively, and the coordinates of its centre are equal to $x = c$, $y = -h (h > 0)$. Rotational oscillations occur with respect to the point $x_0 = c$, $y_0 = -h$ in (2.6). We will consider ice sheets as floating elastic plates. The following values are used for model parameters:

$$\left.\begin{aligned} E = 5\ \text{GPa}, \quad \rho = 922.5\ \text{kg m}^{-3}, \quad \nu = 0.3, \quad \rho_0 = 1025\ \text{kg m}^{-3}, \\ d = 2\ \text{m}, \quad b = 10\ \text{m}, \quad a = h = 20\ \text{m}, \quad H = 500\ \text{m}. \end{aligned}\right\} \tag{5.1}$$

In order to solve the integral equation (3.27) the method of boundary elements is used. The body contour S is divided into N elements. An additional middle point inside each of the elements is introduced and the distribution of an unknown quantity is approximated by a quadratic function of the arc coordinate. Fragmentation of the contour S occurs in such a way that none of the input points does not belong to the boundary between the subdomains Γ_i and Γ_{i+1} $(i = 1, 2)$. Thus, we should solve a $2N$th-order system of linear equations for each $j = 1, 2, 3$ to determine the values of σ_j in all nodal points of the contour S. Only the right-hand side of this system depends on the number j.

The numerical integration in (3.27) is carried out using the Gauss six-point integration formula. At each of these points, the value of the Green's function is determined using the reduction method. Only M of the first terms is taken into account in series (3.3), (3.5), (3.20), and $M + 2$ of the first terms is taken into account in series (3.4), (3.19), (3.21). In each case, the total number of unknown constants R_m, C_m, S_m, T_m is equal to $4M + 8$. The matching conditions (3.16*a*,*b*) and (3.16*c*,*d*) must be satisfied integrally. For the case of finite elastic plate, substituting expansions (3.3) and (3.4) in the first equation (3.16*a*,*b*), multiplying both sides of the equation by $f(y, k_0)$ and $\psi(y, k_m)(m = 1, \ldots, M)$ and integrating the result in y from $-H$ to 0, we arrive at a system of $M+1$ linear algebraic equations. The same is done for the second equation in (3.16*a*,*b*), and we obtain another set of $M + 1$ equations. Substituting expansions (3.4) and (3.5) in the first and second equations (3.16*c*,*d*) and carrying out the same steps as for (3.16*a*,*b*), we obtain another set of $2M + 2$ equations. As a result, we obtain a system of $4M + 4$ linear algebraic equations which must be supplemented with four equations following from substitution of (3.4) into free-edge conditions (2.10). Thus, the total number of equations is equal to the number of the unknown constants $4M + 8$.

The right-hand side of the resulting system of linear algebraic equations contains singular integrals by virtue of the integral representation of functions G_f and G_p in (3.9) and (3.13), respectively. To calculate the singular integral as

$$J \equiv \int_a^b \frac{f(x)}{g(x)}\,\mathrm{d}x, \tag{5.2}$$

where the integrand has only a simple pole at $x = x_0$ $(a < x_0 < b)$, i.e. $g(x_0) = 0$ and $f(x_0) \neq 0$, can be used next representation

$$J = \int_a^b \left[\frac{f(x)}{g(x)} - \frac{f(x_0)}{g'(x_0)(x - x_0)}\right]\mathrm{d}x + \frac{f(x_0)}{g'(x_0)}\int_a^b \frac{\mathrm{d}x}{x - x_0}. \tag{5.3}$$

Now the integrand of the first integral in (5.3) has no singularities, and the second integral is equal to

$$\int_a^b \frac{\mathrm{d}x}{x - x_0} = \ln\left(\frac{b - x_0}{x_0 - a}\right). \tag{5.4}$$

In the case of polynya, the problem is solved in a similar way. Numerical convergence of results obtained by the method MEE is shown in table 1 for the case of the finite elastic platform. The dimensionless coefficients of the radiation load μ_{22}^* and λ_{22}^* (5.5) are given at $L/b = 30$, $c/b = 5$, $\Omega b = 2$. We see that using $N = 20$ and $M = 90$ produce three-significant-figure accuracy. In the numerical results given below, these values N and M are used.

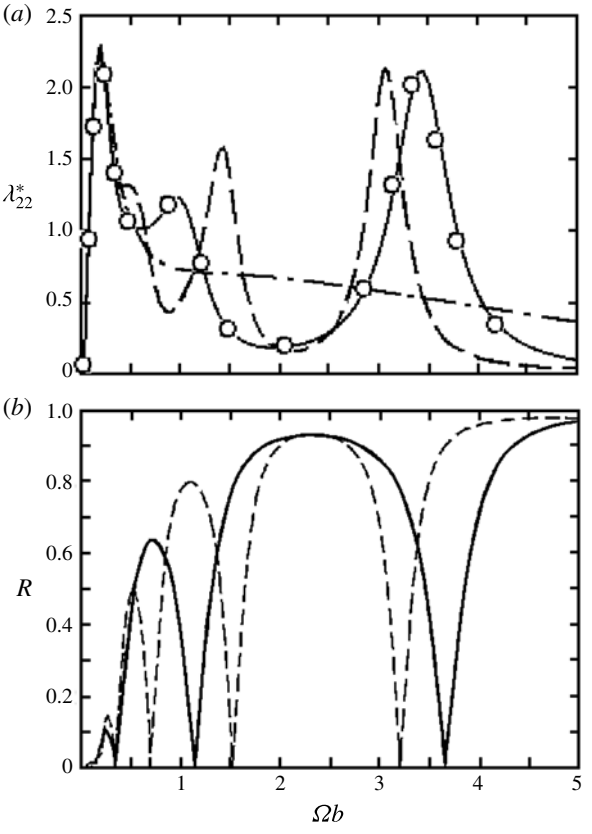

FIGURE 2. (*a*) Heave damping coefficient for the cylinder submerged at $c/b = 5$ underneath the platform with the length $L/b = 19$ (solid line) and $L/b = 30$ (dashed line). The dash-dotted line is for the semi-infinite elastic plate, and open circles are the results of Tkacheva (2015) at $L/b = 19$ obtained with using WHT. (*b*) Reflection coefficient for the finite elastic platform with the length $L/b = 19$ (solid line) and $L/b = 30$ (dashed line).

The calculations of radiation load as function of the oscillation frequency of the elliptical cylinder were given by Tkacheva (2015) in the case of a finite platform at $L/b = 15, 19$ and $c/b = -7, 0, 5$ using WHT and input data (5.1). A comparison of the results WHT and MEE at $L/b = 15$ and $c/b = 5$ was shown by Sturova & Tkacheva (2015). Good agreement of the numerical results of these two methods makes us more confident of the MEE results which are produced. The radiation load matrix is completely filled in the problem under consideration, whereas for an infinitely extended free surface or elastic plate, only the diagonal coefficients τ_{jj} ($j = 1, 2, 3$) and $\tau_{13} = \tau_{31}$ in (4.1) are non-zero.

The greatest influence of finite length of the platform takes place if the body is submerged underneath the platform. Figure 2(*a*) shows the dimensionless damping coefficient λ^*_{22} (5.5) as a function of dimensionless frequency $\Omega b = \omega^2 b/g$ at $c/b = 5$. The results for two ice floes of lengths $L/b = 19$ and $L/b = 30$ are compared with the results for the semi-infinite elastic plate (Sturova 2014). It is known that the resonance frequencies exist for the floating elastic platform are subject to incident wave forcing (e.g. Meylan & Tomic 2012). For diffraction problem (see appendix A), the resonance frequencies correspond to frequencies at which the reflection coefficient

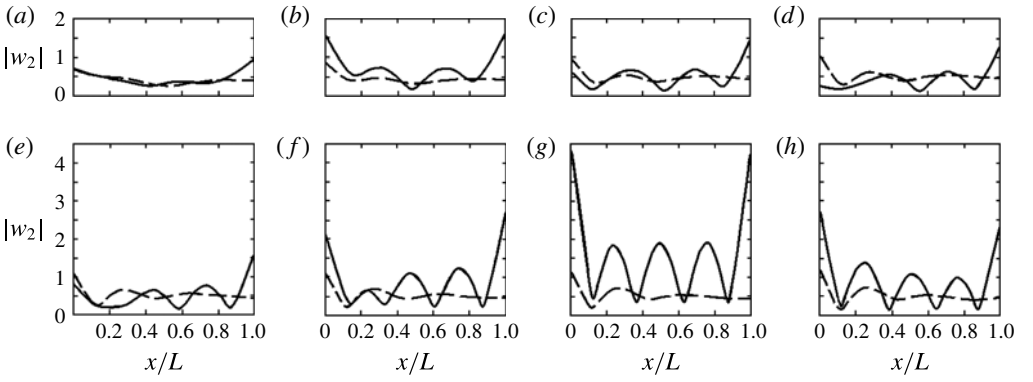

FIGURE 3. Plate deflection amplitudes $|w_2|$ generated by vertical oscillations of the cylinder at $c/b = 5$. The solid lines are for the finite elastic platform with the length $L/b = 19$ and the dashed lines are for the semi-infinite plate. (*a*) $\Omega b = 0.5$; (*b*) $\Omega b = 1$; (*c*) $\Omega b = 1.5$; (*d*) $\Omega b = 2$; (*e*) $\Omega b = 2.5$; (*f*) $\Omega b = 3$; (*g*) $\Omega b = 3.5$; (*h*) $\Omega b = 4$.

M	$N = 10$		$N = 15$		$N = 20$		$N = 25$	
	μ^*_{22}	λ^*_{22}	μ^*_{22}	λ^*_{22}	μ^*_{22}	λ^*_{22}	μ^*_{22}	λ^*_{22}
10	3.1050	0.17322	3.1070	0.17327	3.1072	0.17327	3.1073	0.17328
30	3.1727	0.17335	3.1746	0.17341	3.1749	0.17342	3.1749	0.17342
50	3.1860	0.17285	3.1879	0.17291	3.1882	0.17292	3.1882	0.17292
70	3.1902	0.17275	3.1922	0.17281	3.1924	0.17282	3.1925	0.17282
90	3.1920	0.17271	3.1940	0.17278	3.1943	0.17278	3.1943	0.17279

TABLE 1. Convergence of values of μ^*_{22} and λ^*_{22} with N and M for the case of finite elastic platform at $L/b = 30$, $c/b = 5$, $\Omega b = 2$.

is zero. Figure 2(*b*) presents the reflection coefficient R as a function of frequency at $L/b = 19$ and $L/b = 30$. This figure shows the existence of zeros of R for discrete values of frequency. The number of zeros increases when the length of the platform L increases. Comparison of figures 2(*a*) and 2(*b*) shows that the peaks of the damping coefficient λ^*_{22} occur at frequencies which correspond to zero reflection for both values of length of the platforms.

Figure 3 shows the plate deflection amplitudes $|w_2|$ generated by vertical oscillations of the cylinder at frequencies $\Omega b = 0.5$, 1, 1.5, 2, 2.5, 3, 3.5 and 4. The cylinder is submerged underneath the plate at $c/b = 5$. The results for the finite platform at $L/b = 19$ are compared with the similar results for the semi-infinite plate. We can see that the behaviour of the elastic plates is very different in these two cases. For the finite platform, a sharp increase in plate oscillations occurs in the vicinity of the resonance frequencies at $\Omega b = 1$ and $\Omega b = 3.5$. As follows from the solution of the diffraction problem (see figure 2*b*), the resonance frequencies are approximately equal to $\Omega b \approx 1.14$ and $\Omega b \approx 3.65$. The maximum deflections are achieved at the free edges of the elastic platform.

Consider next the influence of polynya on the wave motion generated by an oscillating submerged cylinder. Figures 4 and 5 present the radiation load for a cylinder submerged under polynya at $L/b = 10$ and $c/b = 5$ as a function of frequency. A sketch of the geometry is shown in figure 4(*a*). The dimensionless radiation load

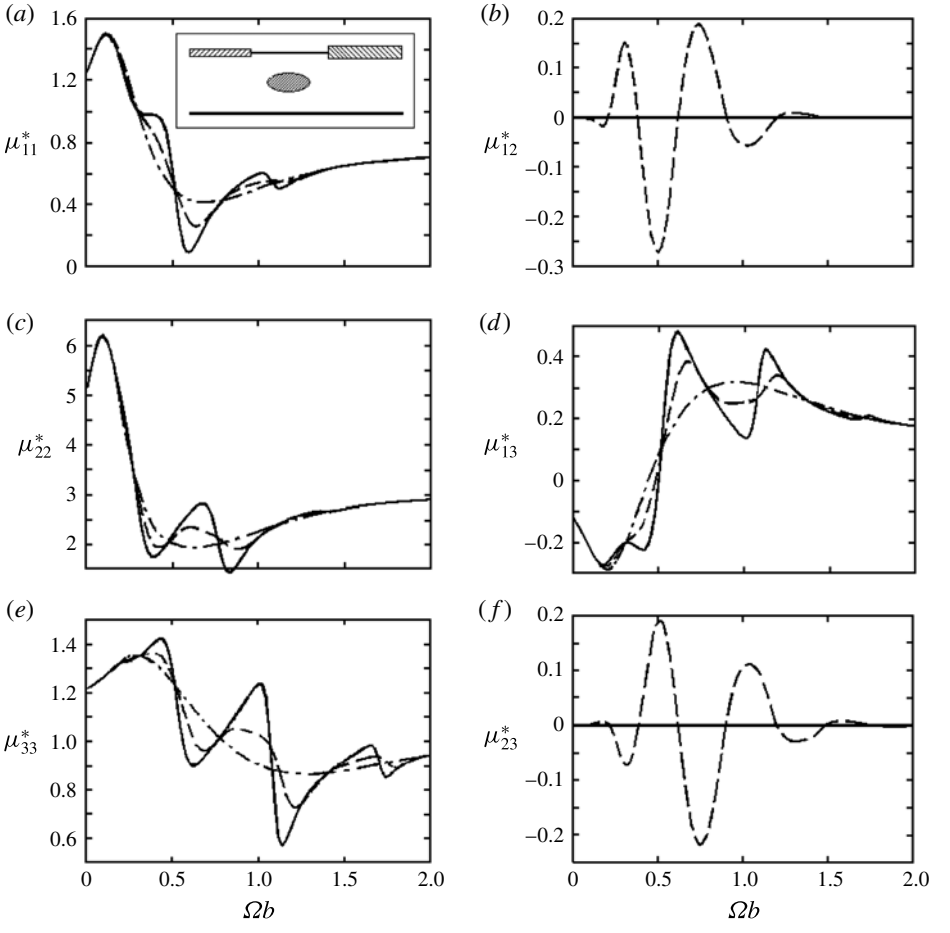

FIGURE 4. Added mass coefficients: (diagonal), (*a*) sway; (*c*) heave; (*e*) roll; (off-diagonal), (*b*) sway–heave; (*d*) sway–roll; (*f*) heave–roll for the cylinder submerged under the polynya at $L/b = 10$, $c/b = 5$ and $d_2 = 2$ m. The solid lines are for the identical plates ($d_1 = d_2$), the dashed lines are for the non-identical ones ($d_1 = 0.5$ m), and the dash-dotted lines are for infinitely extended free surface.

coefficients are introduced as follows:

$$\left.\begin{gathered}\mu^*_{kj} = \frac{\mu_{kj}}{\pi\rho_0 b^2}, \quad \lambda^*_{kj} = \frac{\lambda_{kj}}{\pi\rho_0\omega b^2}, \quad \mu^*_{k3} = \frac{\mu_{k3}}{\pi\rho_0 b^3}, \quad \lambda^*_{k3} = \frac{\lambda_{k3}}{\pi\rho_0\omega b^3} \quad (k, j = 1, 2), \\ \mu^*_{33} = \frac{\mu_{33}}{\pi\rho_0 b^4}, \quad \lambda^*_{33} = \frac{\lambda_{33}}{\pi\rho_0\omega b^4}.\end{gathered}\right\} \tag{5.5}$$

Three cases are compared: the elastic plates are the same ($d_1 = d_2 = 2$ m), the elastic plates have different thicknesses ($d_1 = 0.5$ m, $d_2 = 2$ m) and infinitely extended free surface. As a consequence of symmetry, we have $\tau_{12} = \tau_{23} = 0$ in (4.1) for the first and third cases. The oscillations of the coefficients of radiation load occur near the curves for an infinitely extended free surface. For low and high frequencies, the difference between the three cases is small.

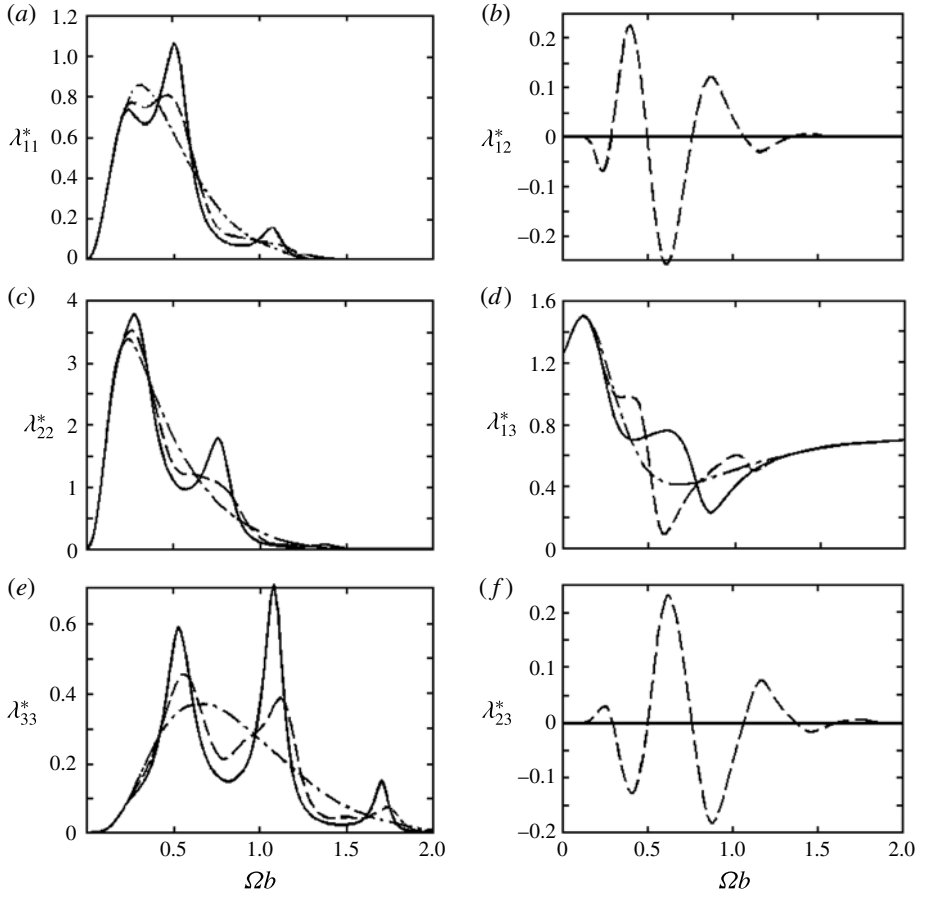

FIGURE 5. As figure 4 but for the damping coefficients.

The most noticeable difference in the maximum values of the diagonal damping coefficients takes place for rotational oscillations of the cylinder. Figure 6 shows vertical displacement amplitudes $|w_3|$ of the free surface generated by oscillations of the cylinder at frequencies $\Omega b = 0.25$, 0.5, 0.75, 1, 1.25, 1.5, 1.75 and 2. At low frequency $\Omega b = 0.25$, the behaviour of the free surface for all three cases is the same, but with increasing frequency differ significantly. For the considered frequencies, the largest displacements of the fluid in polynya arises in the case of identical plates at $\Omega b = 1.75$.

The solution of the diffraction problem on polynya is given in appendix B. Figure 7 shows the reflection coefficient R as a function of frequency at $L/b = 10$ for the identical plates ($d_1 = d_2 = 2$ m) and non-identical ones: ($d_1 = 0.5$ m, $d_2 = 2$ m) and ($d_1 = 2$ m, $d_2 = 0.5$ m). It is seen that in the latter two cases, the values of the reflection coefficient are very close. As noted by Chung & Linton (2005) for identical plates, there are an infinite number of discrete frequencies at which reflection is zero. The curves appear not to reach zero, but this is simply a facet of the resolution in frequency used. All the curves for the magnitude of the reflection coefficient that were presented in that paper for zero incident wave angle are confirmed fully using the present method. For non-identical plates, in comparison with the identical ones,

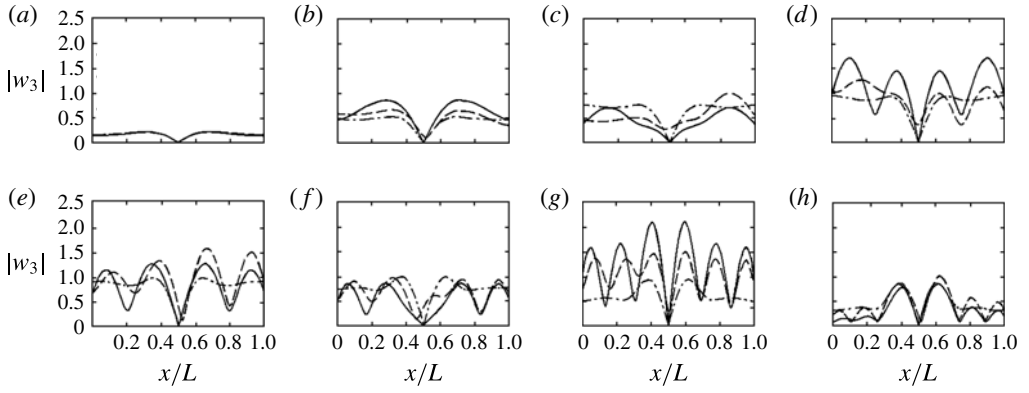

FIGURE 6. Vertical displacement amplitudes $|w_3|$ of the free surface generated by rotational oscillations of the cylinder at $L/b = 10$, $c/b = 5$ and $d_2 = 2$ m. The solid lines are for the identical plates ($d_1 = d_2$), the dashed lines are for the non-identical ones ($d_1 = 0.5$ m), and the dash-dotted lines are for infinitely extended free surface ($\Omega b = 0.25$ (a), 0.5 (b), 0.75 (c), 1 (d), 1.25 (e), 1.5 (f), 1.75 (g), 2 (h)).

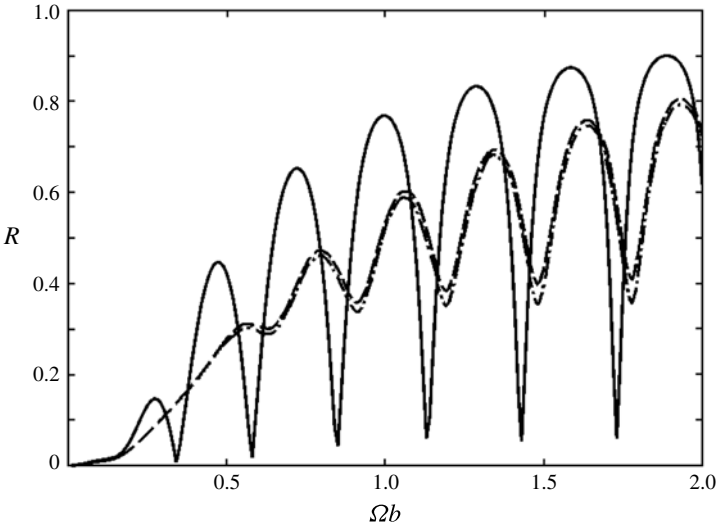

FIGURE 7. Reflection coefficient R as a function of frequency for the polynya with the length $L/b = 10$. The solid line is for the identical plates ($d_1 = d_2 = 2$ m), the dashed and dash-dotted lines are for the non-identical plates ($d_1 = 0.5$ m, $d_2 = 2$ m) and ($d_1 = 2$ m, $d_2 = 0.5$ m), respectively.

local maxima of the reflection coefficient significantly decrease and increase the value of local minima. The frequencies at which radiation load has local extrema in figures 4 and 5 to some degree correspond to the frequencies at which there are local extrema of the reflection coefficient in figure 7. The amplification of fluid oscillations in polynya at $\Omega b = 1.75$ (figure 6) can be explained by the fact that the reflection coefficient R (figure 7) has a local minimum in the vicinity of this frequency.

Figures 8 and 9 present the radiation load for a cylinder submerged underneath the right plate at $L/b = 3$ and $c/b = 8$. A sketch of the geometry is shown in figure 8(a). The cases of identical ($d_1 = d_2 = 2$ m) and non-identical ($d_1 = 0.5$ m, $d_2 = 2$ m)

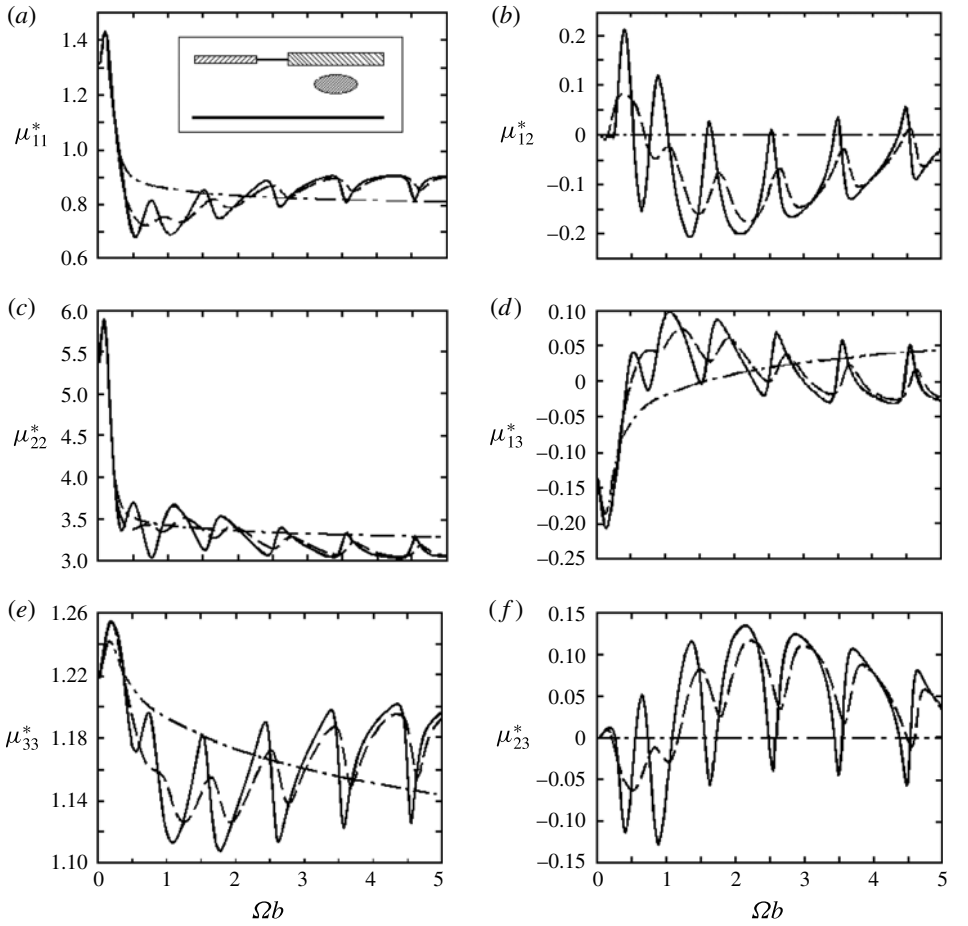

FIGURE 8. Added mass coefficients: (diagonal), (*a*) sway; (*c*) heave; (*e*) roll; (off-diagonal), (*b*) sway–heave; (*d*) sway–roll; (*f*) heave–roll for the cylinder submerged underneath the right plate in the case of polynya at $L/b = 3$, $c/b = 8$ and $d_2 = 2$ m. The solid lines are for the identical plates ($d_1 = d_2$), the dashed lines are for the non-identical plates ($d_1 = 0.5$ m), and the dash-dotted lines are for infinitely extended elastic plate.

plates, as well as an infinitely extended uniform ice cover with thickness 2 m, are compared. As a consequence of symmetry, we have $\tau_{12} = \tau_{23} = 0$ in (4.1) for infinitely extended ice cover. It can be seen that the most noticeable oscillatory dependence of the radiation load on the frequency is shown in the case of identical plates. The presence of open water can both increase and decrease the radiation load compared with infinitely extended ice cover.

Figure 10 shows the vertical displacement amplitudes $|w_2|$ of the elastic plates and free surface at $L/b = 3$ and $c/b = 8$ for the identical plates ($d_1 = d_2 = 2$ m) and non-identical ones ($d_1 = 0.5$ m, $d_2 = 2$ m) at frequencies $\Omega b = 0.5$, 1, 1.5, 2, 2.5, 3, 3.5 and 4. It is interesting that the right plate deflections are in close agreement for the two cases considered, and the left plate deflections are somewhat larger in the case of non-identical plates. However, the displacements of the free surface at certain frequencies differ sharply. As is seen from figure 10, the amplitude of the wave elevation in the gap becomes large. This is due to resonance of the wave in the gap.

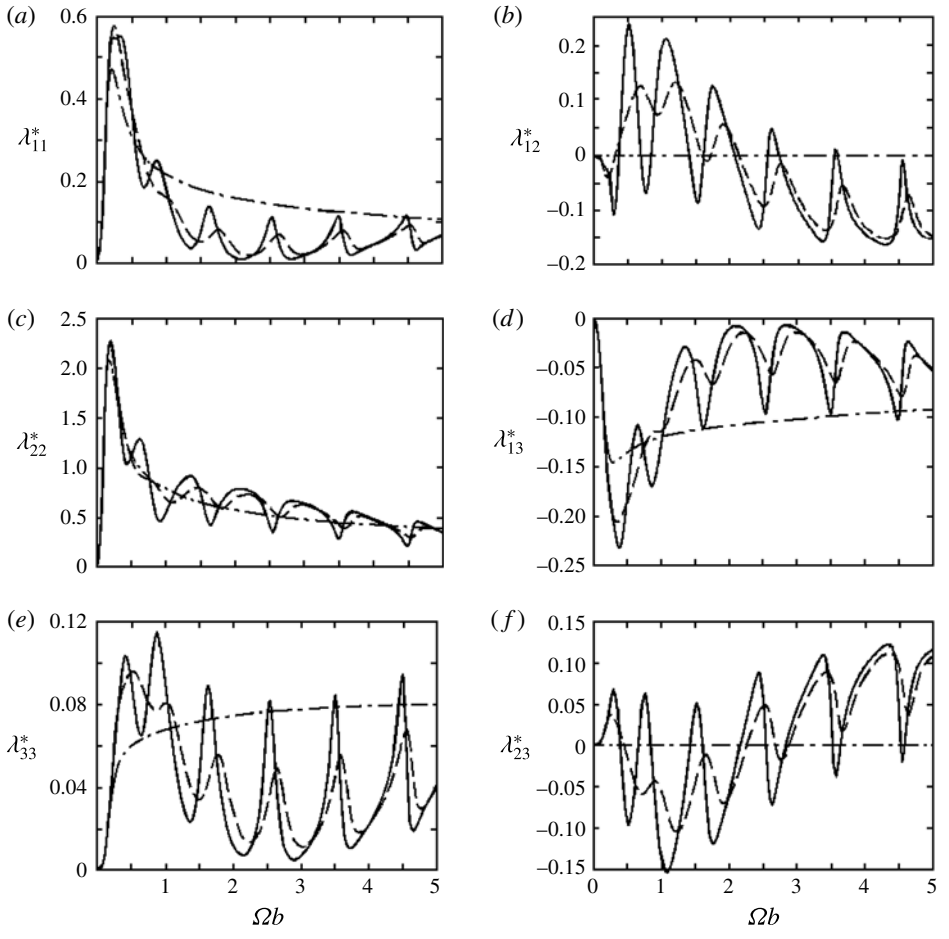

FIGURE 9. As figure 8 but for the damping coefficients.

A similar phenomenon also occurs at the solution of the linear diffraction problem about the interaction of free-surface waves with floating flexible strips separated by a channel of water (e.g. Hermans 2004). In solving these problems in a more complete manner, waves splashing over the deck of the platform should be taken into account, although this is a much more complicated problem than the one covered in this paper.

The maximal values of the vertical displacement amplitudes $\max|w_j|$ in open water at $L/b = 3$ and $c/b = 8$ are shown in figures 11(*a*) and 11(*b*) for the identical plates ($d_1 = d_2 = 2$ m) and non-identical ones ($d_1 = 0.5$ m, $d_2 = 2$ m), respectively. In both cases, the largest free surface displacements have occurred at the vertical oscillations of a cylinder ($j = 2$), and the lowest ones at the rotational oscillations of a cylinder ($j = 3$). Figure 11(*c*) shows the reflection coefficient R for the diffraction problem (appendix B) as function of frequency at $L/b = 3$ for the identical plates ($d_1 = d_2 = 2$ m) and non-identical ones: ($d_1 = 0.5$ m, $d_2 = 2$ m) and ($d_1 = 2$ m, $d_2 = 0.5$ m). It can be seen that the local maxima of $\max|w_j|$ occur at those frequencies at which the reflection coefficient R has local minima, regardless of the type of oscillations of the cylinder. For all calculations, reciprocity relations (4.8*a*,*b*), (4.10), (4.11) were fulfilled with a relative error not greater than 1 %.

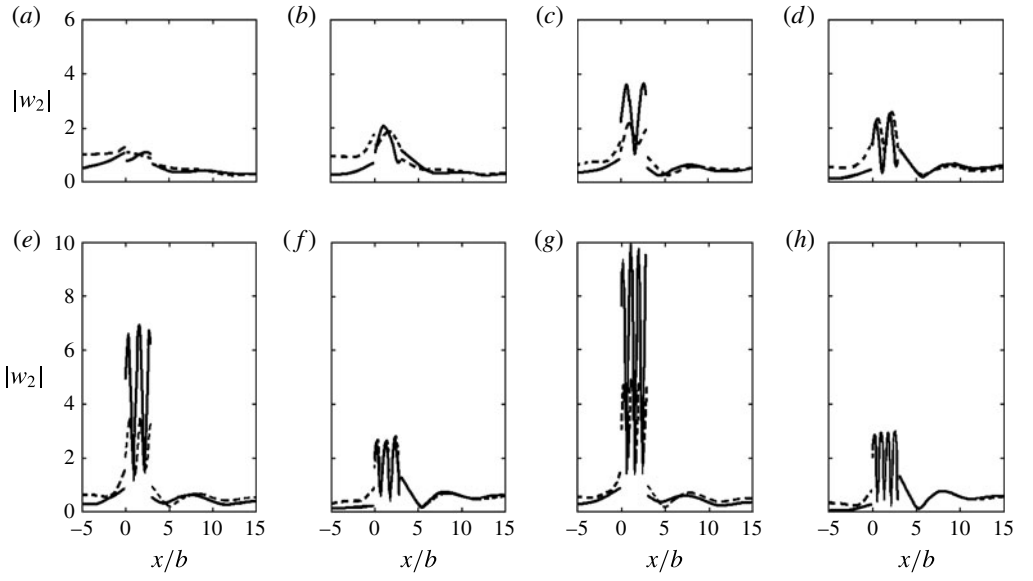

FIGURE 10. Vertical displacement amplitudes $|w_2|$ of the elastic plates and free surface generated by vertical oscillations of the cylinder at $L/b = 3$, $c/b = 8$ and $d_2 = 2$ m. The solid lines are for the identical plates ($d_1 = d_2$) and the dashed lines are for the non-identical plates ($d_1 = 0.5$ m) ($\Omega b = 0.5$ (*a*), 1 (*b*), 1.5 (*c*), 2 (*d*), 2.5 (*e*), 3 (*f*), 3.5 (*g*), 4 (*h*)).

6. Conclusion

Within the framework of linearized theory, the two-dimensional problem of wave motion generated by oscillations of a rigid submerged body has been solved. Two classes of geometry are considered, both involving a fluid domain of infinite extent that is partially covered by a floating thin-elastic plate. In one case, the covering is finite, representing an ice floe, and in the second one, the covering is two semi-infinite elastic plates separated by a region of open water (polynya). The solution is written as a distribution of mass sources over the surface of the body and an integral equation used for the unknown source strength. The corresponding Green's function is constructed using MEE. The radiation load and the amplitudes of vertical displacement of the free surface and elastic plates are calculated. It is shown that the wave motion essentially depends on the position of the submerged body relative to the elastic plate edges. Reciprocity relations which demonstrate both symmetry of the radiation load coefficients and the relation of damping coefficients with the far-field form of the radiation potentials are found. The results of solving the radiation problem are compared with the solution of the diffraction problem. It is noted that the resonant frequencies in the radiation problem correlate with those frequencies at which the reflection coefficient in the diffraction problem has a local minimum. The approach proposed in this paper can be extended to the case of a three-dimensional submerged body. It is the author's opinion that the simplest problem is the radiation problem of a sphere submerged under a floating semi-infinite elastic plate.

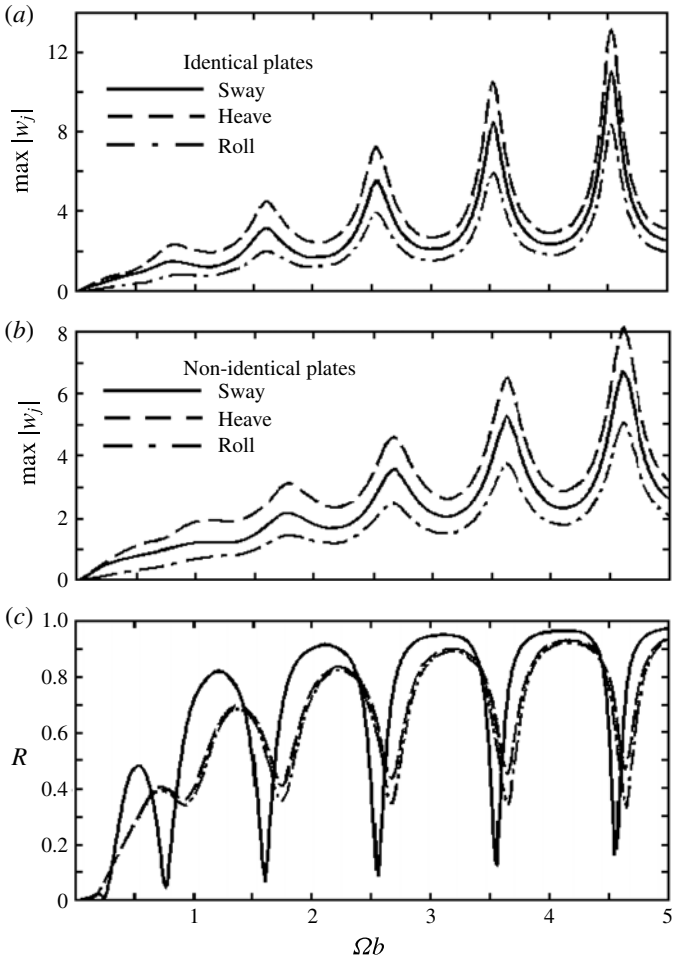

FIGURE 11. Maximal values of the vertical displacement amplitudes max $|w_j|$ of sway ($j=1$), heave ($j=2$) and roll ($j=3$) as a function of frequency at $L/b=3$, $c/b=8$ and $d_2=2$ m: (*a*) identical plates ($d_1=d_2$); (*b*) non-identical plates ($d_1=0.5$ m). (*c*) Reflection coefficient R as a function of frequency for the polynya with the length $L/b=3$. The solid line is for the identical plates ($d_1=d_2=2$ m), the dashed and dash-dotted lines are for the non-identical plates ($d_1=0.5$ m, $d_2=2$ m) and ($d_1=2$ m, $d_2=0.5$ m), respectively.

Acknowledgements

I am grateful to the anonymous referees whose comments resulted in a considerable improvement of the original manuscript.

Appendix A. Surface wave diffraction on a floating elastic platform

The problem of two-dimensional floating elastic plate of finite length and zero draft is the simplest and best-studied problem in hydroelasticity. At the present time, there are many methods for solving this problem. Extensive literature can be found in Squire (2011) and Sahoo (2012). The most simple method is based on the use of MEE. The solution of this problem is outlined below.

Let us assume that at the free surface of a fluid layer of depth H there is freely floating elastic platform of width L, uniform mass density ρ and thickness d. The

fluid–structure system is similar to that shown in figure 1(*a*) except for the submerged cylinder. A train of surface gravity waves propagates from left to right. The incoming wave is sinusoidal in time with angular frequency ω and wavenumber k_0. Then its velocity potential can be expressed by

$$\Phi_0(x, y, t) = \mathrm{Re}\{f(y, k_0)\exp[\mathrm{i}(\omega t - k_0 x)]\}, \tag{A 1}$$

where notation (3.6*a*,*b*) and (3.7) is used. The resulting velocity potential can be presented as follows:

$$\Phi(x, y, t) = \mathrm{Re}[\varphi(x, y)\exp(\mathrm{i}\omega t)]. \tag{A 2}$$

In order to determine the function $\varphi(x, y)$ the boundary-value problem should be solved similarly to (2.4), (2.7)–(2.10). Using the results of § 3.1, the value of $\varphi(x, y)$ in the subdomain Γ_i is denoted $\varphi_i(x, y)$ $(i = 1, 2, 3)$ and can be found in the form:

$$\varphi_1 = (\mathrm{e}^{-\mathrm{i}k_0 x} + R_0\mathrm{e}^{\mathrm{i}k_0 x})f(y, k_0) + \sum_{m=1}^{\infty} R_m \mathrm{e}^{k_m x}\psi(y, k_m) \quad (x, y \in \Gamma_1), \tag{A 3}$$

$$\varphi_2 = [C_0\mathrm{e}^{-\mathrm{i}s_0 x} + S_0\mathrm{e}^{\mathrm{i}s_0(x-L)}]f(y, s_0) + \sum_{\substack{m=-2\\ m\neq 0}}^{\infty} [C_m\mathrm{e}^{-s_m x} + S_m\mathrm{e}^{s_m(x-L)}]\psi(y, s_m) \quad (x, y \in \Gamma_2), \tag{A 4}$$

$$\varphi_3 = T_0\mathrm{e}^{\mathrm{i}k_0(L-x)}f(y, k_0) + \sum_{m=1}^{\infty} T_m\mathrm{e}^{k_m(L-x)}\psi(y, k_m) \quad (x, y \in \Gamma_3). \tag{A 5}$$

The system of linear algebraic equations for determining the unknown constants R_m, C_m, S_m, T_m is obtained analogously to § 5.

The quantities R_0 and T_0 are called the reflection and transmission coefficients and satisfy the well-known energy flux condition

$$R^2 + T^2 = 1, \quad R = |R_0|, \quad T = |T_0|. \tag{A 6a–c}$$

Appendix B. Wave propagation across a polynya

It will be assumed that two thin semi-infinite elastic plates with different properties freely float on the surface of the fluid. There is a finite gap of free surface between these plates. The fluid–structure system is similar to that shown in figure 1(*b*) except for the submerged cylinder. Previously, this problem was solved by Chung & Linton (2005) for identical plates and Chakrabarti & Mohapatra (2013) for non-identical ones. In the first paper, the method of solution was based on the residue calculus technique. In the second paper, the method of least squares as well as singular value decomposition have been employed.

The potential for flexural-gravity wave incoming from the left infinity becomes

$$\Phi_0(x, y, t) = \mathrm{Re}\{f(y, q_0)\exp[\mathrm{i}(\omega t - q_0 x)]\}, \tag{B 1}$$

where notation (3.6*a*,*b*) and (3.22*a*) is used. The resulting velocity potential can be written in the form (A 2). For determination of the function $\varphi(x, y)$, the boundary-value

problem should be solved similarly to § 3.2 and the value of $\varphi(x, y)$ in the subdomains Γ_i can be found in the form

$$\varphi_1 = (\mathrm{e}^{-\mathrm{i}q_0 x} + R_0 \mathrm{e}^{\mathrm{i}q_0 x}) f(y, q_0) + \sum_{\substack{m=-2 \\ m\neq 0}}^{\infty} R_m \mathrm{e}^{q_m x} \psi(y, q_m) \quad (x, y \in \Gamma_1), \tag{B 2}$$

$$\varphi_2 = [C_0 \mathrm{e}^{-\mathrm{i}k_0 x} + S_0 \mathrm{e}^{\mathrm{i}k_0 (x-L)}] f(y, k_0) + \sum_{m=1}^{\infty} [C_m \mathrm{e}^{-k_m x} + S_m \mathrm{e}^{k_m (x-L)}] \psi(y, k_m) \quad (x, y \in \Gamma_2), \tag{B 3}$$

$$\varphi_3 = T_0 \mathrm{e}^{\mathrm{i}p_0 (L-x)} f(y, p_0) + \sum_{\substack{m=-2 \\ m\neq 0}}^{\infty} T_m \mathrm{e}^{p_m (L-x)} \psi(y, p_m) \quad (x, y \in \Gamma_3). \tag{B 4}$$

Using the results of § 4, the energy flux condition can be expressed

$$R^2 + \Upsilon_2 T^2 / \Upsilon_1 = 1, \quad R = |R_0|, \, T = |T_0|, \tag{B 5}$$

where the values Υ_1 and Υ_2 are given in (4.12*a*,*b*). In the case of identical plates, energy identity (B 5) has the form (A 6*a*–*c*).

Energy-balance relation for non-identical plates was given by Chakrabarti & Mohapatra (2013) in the form

$$R^2 + QT^2 = 1, \tag{B 6}$$

where

$$Q = \frac{p_0 \tanh p_0 H \cosh^2 q_0 H}{q_0 \tanh q_0 H \cosh^2 p_0 H} \left[\frac{2p_0 H (D_2 p_0^4 + 1 - \Omega B_2) + (5 D_2 p_0^4 + 1 - \Omega B_2) \sinh 2p_0 H}{2q_0 H (D_1 q_0^4 + 1 - \Omega B_1) + (5 D_1 q_0^4 + 1 - \Omega B_1) \sinh 2q_0 H} \right]. \tag{B 7}$$

It can be shown that (B 5) and (B 6) coincide. It is interesting to note that the energy identity (B 6) was obtained by Barrett & Squire (1996) for the problem of propagation of flexural-gravity waves across an abrupt change of properties within a continuous ice sheet.

REFERENCES

Barrett, M. D. & Squire, V. A. 1996 Ice-coupled wave propagation across an abrupt change in ice rigidity, density, or thickness. *J. Geophys. Res.* **101**, 20825–20832.

Chakrabarti, A. & Mohapatra, S. 2013 Scattering of surface water waves involving semi-infinite floating elastic plates on water of finite depth. *J. Mar. Sci. Appl.* **12**, 325–333.

Chung, H. & Linton, C. M. 2005 Reflection and transmission of waves across a gap between two semi-infinite elastic plates on water. *Q. J. Mech. Appl. Maths* **58**, 1–15.

Fox, C. & Squire, V. A. 1994 On the oblique reflexion and transmission of ocean waves at shore fast sea ice. *Phil. Trans. R. Soc. Lond.* A **347**, 185–218.

Hermans, A. J. 2004 Interaction of free-surface waves with floating flexible strips. *J. Engng Maths* **49**, 133–147.

Hermans, A. J. 2014 The interaction of a submerged object with a very large floating platform. In *Proceedings of the 29th International Workshop on Water Waves and Floating Bodies, Osaka, Japan, March 30–April 02*.

LINTON, C. M. & MCIVER, P. 2001 *Handbook of Mathematical Techniques for Wave/Structure Interactions*. Chapman & Hall/CRC Press.

MEYLAN, M. H. & TOMIC, M. 2012 Complex resonances and the approximation of wave forcing for floating elastic bodies. *Appl. Ocean Res.* **36**, 51–59.

SAHOO, T. 2012 *Mathematical Techniques for Wave Interaction with Flexible Structures*. CRC Press.

SAVIN, A. A. & SAVIN, A. S. 2013 Waves generated on an ice cover by a source pulsating in fluid. *Fluid Dyn.* **48**, 303–309.

SQUIRE, V. A. 2011 Past, present and impendent hydroelastic challenges in the polar and subpolar seas. *Phil. Trans. R. Soc. Lond.* A **369**, 2813–2831.

STUROVA, I. V. 2013 Unsteady three-dimensional sources in deep water with an elastic cover and their applications. *J. Fluid Mech.* **730**, 392–418.

STUROVA, I. V. 2014 Wave generation by an oscillating submerged cylinder in the presence of a floating semi-infinite elastic plate. *Fluid Dyn.* **49**, 504–514.

STUROVA, I. V. 2015 The effect of a crack in an ice sheet on the hydrodynamic characteristics of a submerged oscillating cylinder. *J. Appl. Maths Mech.* **79**, 170–178.

STUROVA, I. V. & TKACHEVA, L. A. 2015 Wave radiation by a cylinder submerged in water with an ice floe or a polynya. In *Proceedings of 30th International Workshop on Water Waves and Floating Bodies, Bristol, UK, April 12–15*.

TKACHEVA, L. A. 2015 Oscillations of submerged cylinder in fluid in the presence of an ice cover. *J. Appl. Mech. Tech. Phys.* (in press).